Materials Chemistry and Physics 163 (2015) 286–292

Contents lists available at ScienceDirect

Materials Chemistry and Physics

journal homepage: www.elsevier.com/locate/matchemphys

New bismuth borophosphate Bi_4BPO_{10}: Synthesis, crystal structure, optical and band structure analysis

Nicolay A. Babitsky [a], Darya Y. Leshok [a], Natalia S. Mikhaleva [a], Aleksandr A. Kuzubov [a, b], Vladimir P. Zhereb [a], Sergei D. Kirik [a, *]

[a] Siberian Federal University, 79 Svobodny Av, Krasnoyarsk, 660041, Russian Federation
[b] Institute of Physics SB RAS, Krasnoyarsk 660036, Russian Federation

HIGHLIGHTS

- New bismuth borophosphate with composition Bi_4BPO_{10} was synthesized.
- The crystal structure was determined by X-ray powder diffraction technique.
- Bismuth-oxygen part $[Bi_4O_3]^{6+}$ forms endless strips of 4 bismuth atoms width.
- Electronic structure was modeled by DFT method.
- The calculated band gap (3.56 eV) is very close to the experimental one (3.46 eV).

GRAPHICAL ABSTRACT

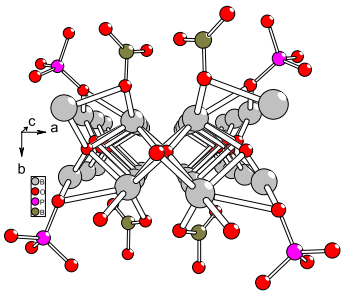

ARTICLE INFO

Article history:
Received 7 September 2014
Received in revised form
10 July 2015
Accepted 14 July 2015
Available online 18 July 2015

Keywords:
Inorganic compounds
Crystal growth
Crystal structure
Band-structure

ABSTRACT

New bismuth borophosphate Bi_4BPO_{10} was obtained by spontaneous crystallization from the melt of correspondent composition at 804 °C. Crystal structure with orthorhombic lattice parameters: a = 22.5731(3) Å, b = 14.0523(2) Å, c = 5.5149(1) Å, V = 1749.34(4), Z = 8, SG Pcab was determined by X-ray powder diffraction technique. The $[Bi_2O_2]^{2+}$ -layers, which are typical for bismuth oxide compounds, transform into cationic endless strips of 4 bismuth atoms width directed along the c-axis in Bi_4BPO_{10}. The strips combining stacks are separated by flat triangle $[BO_3]^{3-}$ -anions within stacks. Neighboring stacks are separated by tetrahedral $[PO_4]^{3-}$-anions and shifted relatively to each other. Bismuth atoms are placed in 5–7 vertex oxygen irregular polyhedra. Bi_4BPO_{10} is stable up to 812 °C, then melts according to the peritectic law. The absorption spectrum in the range 350–700 nm was obtained and the width of the forbidden band was estimated as 3.46 eV. The band electronic structure of Bi_4BPO_{10} was modeled using DFT approach. The calculated band gap (3.56 eV) is in good agreement with the experimentally obtained data.

1. Introduction

Steady interest to bismuth containing mixed oxides is supported over the years due to the variety of phases with interesting physical properties. Crystalline bismuth borates are well known due to

* Corresponding author.
E-mail addresses: alexkuzubov@gmail.com (A.A. Kuzubov), kiriksd@yandex.ru (S.D. Kirik).

http://dx.doi.org/10.1016/j.matchemphys.2015.07.042
0254-0584/

optical activity. Bismuth borate glasses have also found an application in optics. BiB_3O_6 crystals attracted attention by its non-linear optical properties [1]. The phase diagram of Bi_2O_3–B_2O_3 system was firstly described in [2]. There were data on five double oxides with Bi:B ratio 12:1, 2:1, 3:5, 1:3 and 1:4. Later, the data on four polymorphs were added to this number [1]. The existence of six polymorphs of bismuth triborates BiB_3O_6 was reported in [3]. In addition, the metastable diagram was discussed in the literature [4]. Two compounds with Bi:B ratio 5:3 and 1:1 were described.

The data on quasi binary system Bi_2O_3 – $BiPO_4$ were published in [5–7]. It appeared to be very rich for individual phases. The existence from four [5,6] to ten [7] double oxides have been mentioned. For example, the phases with Bi:P ratio 17:1, 7:1, 5,7:1, 31:9, 3:1, 37:13, 17:7, 2:1, 7:4 11:7 were noted in [7].

One compound is known in B_2O_3–P_2O_5 system. It is boron orthophosphate BPO_4, having tetrahedral and hexagonal modifications. The latter melts congruently at 1600 °C.

The abundance of compounds in binary systems is in the contrast with scarcity of the data on the ternary system Bi_2O_3–B_2O_3–P_2O_5. The area near bismuth oxide in composition triangle was described in [8,9] where ternary oxide with sillenite structure was detected. Boron and phosphorus atoms occupy the joint crystallographic positions in the structure. Limited information concerning an existence of two ternary compounds with the compositions $Bi_{9.68}B_{2.58}P_{0.65}O_{20}$ and $Bi_{10}B_6P_2O_{29}$ was reported in [10]. There are no data on ternary bismuth–boron–phosphorus oxides in the current version of ICSD database [version 1.9.4-2014-2]. However, variety of chemical compounds are already established in binary systems causing the assumption of the existence of a number of crystalline phases in the ternary system which detections are difficult for some reasons. The expectation is supported by the extensive surveys dedicated to the synthesis, structure and properties of borophosphates with other elements [11,12].

In this paper practically pure ternary oxide Bi_4BPO_{10} was obtained by the spontaneous crystallization approach. The X-ray powder diffraction data were interpreted and the crystal structure of the phase was established. The temperature range of thermal stability was investigated. The band electronic structure was calculated and its correspondence to obtained spectroscopic data was considered.

2. Materials and methods

2.1. Synthesis of Bi_4BPO_{10}

The synthesis of Bi_4BPO_{10} was carried out with correspondence thermal analysis data. Bi_2O_3 and B_2O_3 (highest purity grade, REAKHIM, RF) have been used as starting chemicals for preparation of initial melt. Phosphorus was introduced into the system in the form of BPO_4, previously prepared according to [13]. Initial reagents were calcined in a platinum crucible: boron oxide – at 1000–1100 °C for 6–10 h, the other components at 700 °C. Starting components were loaded into a platinum crucible, melted at 900 °C and kept at this temperature until complete homogenization. The melt cooling was carried out in several steps. At the first step the melt was cooled down to the intermediate temperature 820 °C with the rate about 5 °C/min and exposed for about an hour. At the second step the melt was cooled down to 806–810 °C with the rate 1–3 °C/h. Then the platinum wire was introduced in the melt as a seed and temperature was gradually adjusted to 800–806 °C. Under these conditions, intergrowth crystals of Bi_4BPO_{10} grew on the platinum wire with the size up to 5 mm. The crystals were taken from the melt and cooled in air. The weight lost of the melt due to evaporation was not higher than 1% in the course of the synthesis.

2.2. Thermal analysis

The simultaneous thermal analyzer Neitzsch STA 449S was used for thermal analysis. The heating rate was 5°/min. Fig. 1 presents the thermograms of initial mixture and Bi_4BPO_{10} heating.

2.3. The spectroscopic data (FT-IR and VIZ)

IR spectra were recorded in the 400–4000 cm^{-1} region with resolution 2 cm^{-1} on Nicolet 6700 IR spectrophotometer (Fig. 2). The sample was prepared by mixing approximately 1 mg of material Bi_4BPO_{10} with 1 g KBr. The resulting mixture was milled and pressed into the tablet.

The absorption spectrum in the visible and UV ranges were obtained on Shimadzu UV-3600 spectrophotometer in the wavelength range 350–700 nm with 1 nm resolution. According to the absorption edge the band gap was determined. Elemental analysis was carried out by EPMA approach using SEM TM3000 (Hitachi) with SwiftED3000 detector (Oxford Instruments Analytical Ltd.).

2.4. Crystal structure determination

The X-ray powder diffraction data were obtained using X'Pert PRO diffractometer (PANalytical) with PIXcel detector, equipped with a graphite monochromator and CuKα radiation. The substance for sample was grinded in an agate mortar and placed in the cuvette of 25 mm diameter by means of direct loading. The excess of the substance was cut off with a razor to prevent particle preferred orientation on the surface. The scan was performed at T = 22 °C in the range from 5 to 110° 2θ, step 0.026°, Δt – 50 °C. The angular limit for the scan was caused by the lack of significant diffraction peak in the far angle region.

Unit cell parameters were determined and refined using the programs described in [14,15]. Approximate bismuth atom locations were established by direct methods using EXPO2004 program [16]. The positions of light atoms were determined on the basis of electron density maps and refined with the help of programs [17,18]. The restrictions as weight coefficients were imposed on refined coordinates to ensure compliance with expected intermolecular geometry (interatomic distances and angles) for known structural groups. The structure refinement was carried out by gradual removal of restrictions. Thermal parameters of bismuth atoms were refined in the anisotropic approximation, others – in the isotropic. The final correspondence between the calculated and experimental X-ray diffraction patterns for the final structural model is shown in Fig. 3. Table 1 summarizes crystallographic data experimental conditions and Figs. 4–6 shows the crystal structure of Bi_4BPO_{10}.

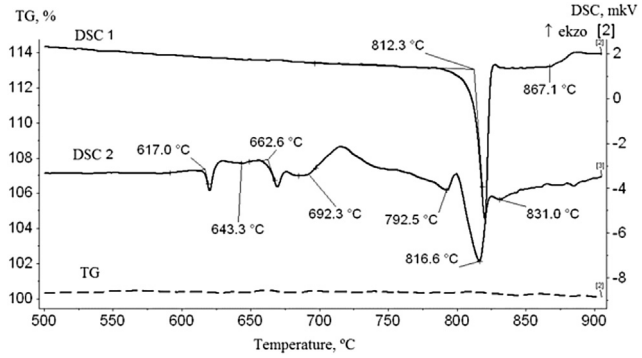

Fig. 1. The heating curves of the sample Bi_4BPO_{10} phase (DSC 1) and the starting mixture Bi_2O_3 and BPO_4 (DSC 2).

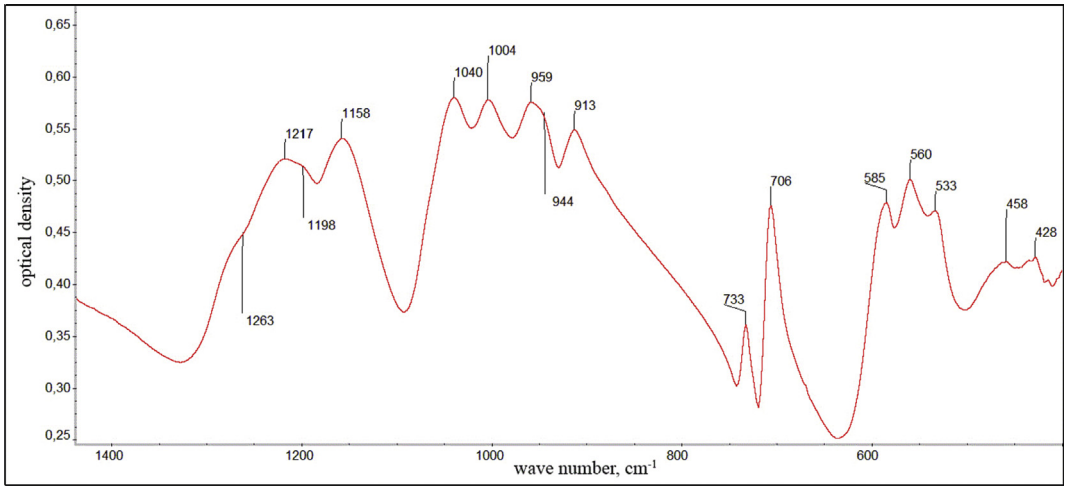

Fig. 2. IR-FT spectrum of the phase Bi_4BPO_{10}.

2.5. Quantum chemical modeling

Quantum chemical modeling of band structure was carried out using the software package VASP 5.2. (Vienna Ab-initio Simulation Package) [19,20]. The density functional theory (DFT) was applied [21,22] with the plane wave basis set and PAW formalism [23,24]. The calculations were carried out using the generalized gradient approximation (GGA) – exchange-correlation functional PBE (Perdew–Burke–Ernzerhof). By optimization of geometry and construction of the states densities for the integration by the first Brillouin zone (1BZ), which was automatically divided into a grid 4·4·6 selected by scheme Monhorsta-Pak [25]. The lattice reciprocal space was divided into 20 intermediate k-points along each symmetry directions for the band structure constructing. The cutoff energy of the plane waves in the calculations was 400 eV. The structure modeling was carried out to maximum values of the forces, acting on atoms, equal to 0.01 eV/Å.

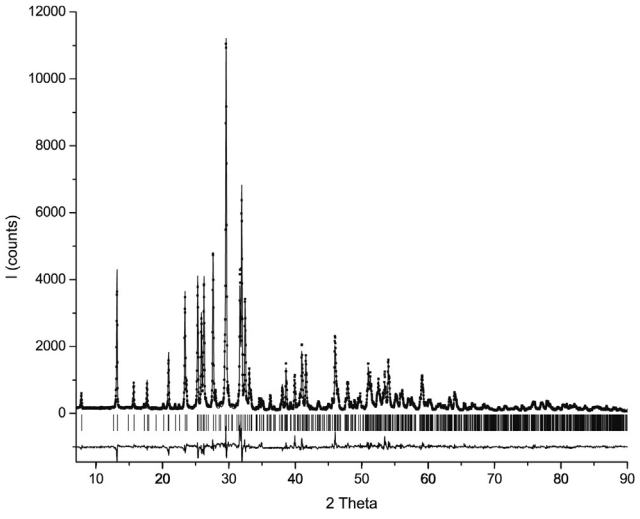

Fig. 3. XRD pattern for Bi_4BPO_{10}. The experimental (dots) and calculated (solid line), the difference (solid line), position of calculated reflections in bottom.

3. Results and discussion

3.1. Phase formation and thermal properties

Studying the system Bi_2O_3–B_2O_3–P_2O_5 it was found that $2Bi_2O_3$:BPO_4 mixture annealing at 700 °C leaded to formation of new ternary oxide Bi_4BPO_{10}. A sample of the same composition obtained by quenching from the melt, followed by annealing, was virtually identical. However, the solid state interaction resulted in the appearance of small impurities including Bi_7PO_{13} (PDF 49–38). When the melt was cooled at rate 5 °C/min a multiphase mixture was formed whose main component was Bi_4BPO_{10} with phases Bi_3PO_7 (PDF 44–645) and $Bi_4B_2O_9$ (PDF 46–420) as impurities. The impurities prevented the phase composition establishing, the crystal structure determination and investigation of physical properties.

Table 1
Crystallographic data and some experimental conditions for Bi_4BPO_{10}.

Chemical formula	Bi_4BPO_{10}
Molecular weight	1037.70
Crystal system	Orthorhombic
Space group	Pcab(61)
A, Å	22.5731(3)
B, Å	14.0523(2)
C, Å	5.51487(8)
α, °	90
β, °	90
γ, °	90
V, Å^3	1749.34(4)
Z	8
$P_{calc.}$, g/cm^3	7.88
Colour	Colorless
μ, mm^{-1}	157.39
T, *K*	295
Diffractometer	X'Pert PRO
Radiation	Cu Kα
λ, Å	$\lambda_1 = 1.54056$, $\lambda_2 = 1.54439$
Scan. area, 2θ (°)	3.014–110.92
Number of points	3192
Number of reflections	1108
Number of refined parameters	96
R_p, %	8.10
R_{wp}, %	10.60
R_{exp}, %	5.70
$S = R_{wp}/R_{exp}$	1.88

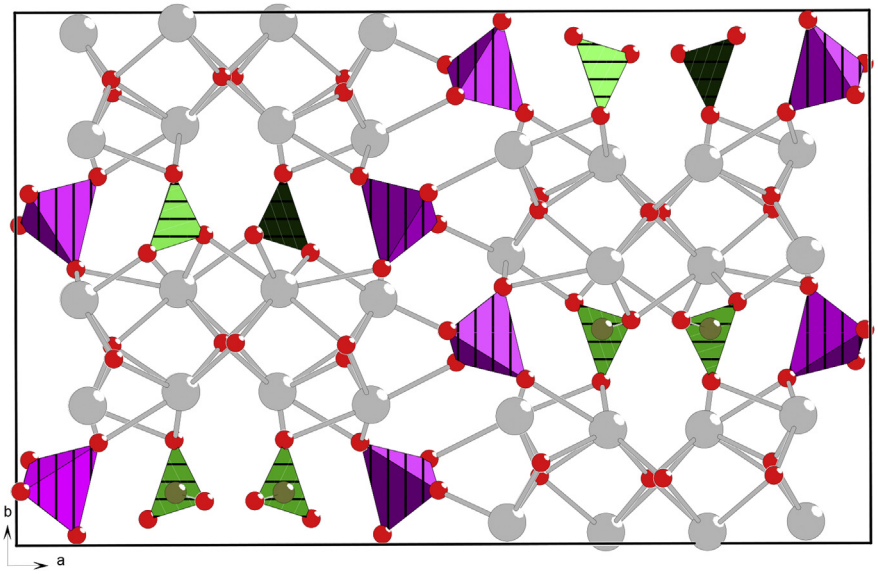

Fig. 4. The crystal structure of Bi_4BPO_{10}.

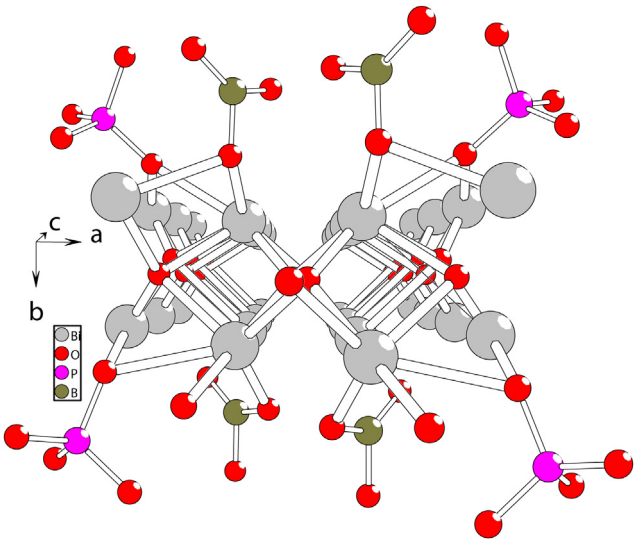

Fig. 5. Bismuth–oxygen tape with composition $[Bi_4O_3]^{6+}$ and coordinating anions $[PO_4]^{3-}$ and $[BO_3]^{3-}$.

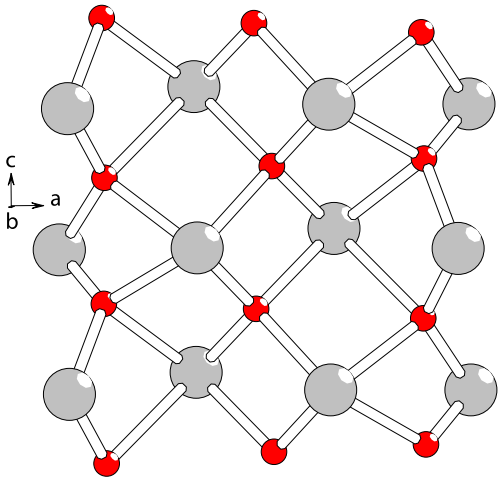

Fig. 6. Bismuth–oxygen tape with composition $[Bi_4O_3]^{6+}{}_n$.

The synthesis approach of the pure phase was selected on basis of thermal analysis data. The thermogram of the original sample with composition $2Bi_2O_3$:BPO_4 has a number of effects caused by the interactions of the initial components (Fig. 1). The endothermic effect is associated with the solidus and solidus on the phase diagram $Bi_2O_3 - B_2O_3$. The appearance of the liquid phase activates the component interactions. The exothermic effect at 692 °C is extended on temperature axis, indicating the diffusion restrictions for the chemical reaction. The exothermic effect at 792 °C quickly transforms into deep endothermic one which corresponds to the peritectic decomposition of Bi_4BPO_{10}. Further heating does not induce any individual thermal effects. It means that the system is being in liquid state. Taking into account specific thermal behavior of the bismuth compound near the melting point, the experience of solid state synthesis and synthesis by annealing the quenched melt, the method of spontaneous crystallization was tested for the single phase material preparation. The melt was prepared as described above. It was cold close to the peritectic temperature and then platinum wire was applied as crystallization seeding. The substance formed on the end of the wire was colorless or yellowish transparent solid with the hardness equals 5 on the Mohs scale. There is only the endothermic peak at 812 °C corresponding peritectic decomposition on the thermogram of the sample. The extended thermal effect covers the temperature associated with the liquidus (Fig. 1). Gravimetric measurements showed the constant weight of the sample during heating up to 1100 °C.

To confirm the chemical composition of the crystals X-ray microprobe analysis was performed. Composition of the sample: 15.23 mas.% O, 80.73 mas.% Bi, 1.27 mas.% B, 2.76 mas.% P (61.6 at.% O, 24.9 at.% Bi, 7.7 at.% B, 5.7 at.% P). Taking into account the e.s.d. of the method we can assert that the compound has a stoichiometric composition Bi_4BPO_{10}.

3.2. IR spectroscopy of Bi_4BPO_{10}

The band assignments in IR spectrum of Bi_4BPO_{10} were made basing on literature data [26–29]. There are four extended

absorption region (Fig. 2). The bands in the range 400–600 cm^{-1} were assigned to the valence vibrations of ν_s(Bi–O) bonds. Absorption bands at 705 cm^{-1} and 730 cm^{-1} in adjacent area can be interpreted as the asymmetric oscillation of bridging bonds in the polymer chains δ_{as}(B–O–Bi) and δ_{as}(P–O–Bi) respectively. Symmetric and asymmetric valence vibrations ν_s,ν_{as}(P–O) give a set of split bands near 1000 cm^{-1} referring to vibrations in the tetrahedral anions PO_4^{3-}. In the region 1150–1300 cm^{-1} there are absorption bands related to boron-oxygen structural units. There are no bands corresponding (B–O–P) vibrations detected on IR spectrum.

3.3. Crystal structure of Bi_4BPO_{10}

Because of the difficulty in obtaining perfect single crystals in conditions of peritectic reaction the crystal structure investigation was carried out by X-ray powder diffraction technique. The basic crystal data and conditions of the diffraction experiment are shown in Table 1. The experimental and calculated X-ray diffraction patterns are shown in comparison in Fig. 3. The degree of diffraction pattern fitness allows us to suppose that the level of possible impurities does not exceed 1–1.5 %.

The crystal structure of Bi_4BPO_{10} can be referred to strip polymers (Fig. 4). Considering symmetry, local structure, bond lengths allows identify the individual anionic groups $[PO_4]^{3-}$ and $[BO_3]^{3-}$ within the crystal framework. They can be regarded as anions compensating charge of cationic part with formal composition $[Bi_4O_3]$ and polymer structure. Anions $[PO_4]^{3-}$ have nearly ideal tetrahedral geometry with the P–O distances in the range 1.51–1.53 Å (Tables 2 and 3). $[BO_3]^{3-}$ anions are slightly distorted planar triangles with B–O distance of about 1.42 Å.

The cationic part of the structure is formed by three layered endless strips $[Bi_4O_3]_n$ oriented along the c-axis (Figs. 5 and 6). Taking into account the charge of phosphate and borate groups the specific charge of the bismuth-oxygen stripe should be regarded as $[Bi_4O_3]^{6+}$. Thus, the positively charged strips are coordinated by phosphate and borate anions. The strip structure presents distorted fragment of a three-layer fluorite-grid $[Bi_2O_2]^{2+}$, well known as δ–Bi_2O_3 structure and occurred in numerous Aurivillius phases [30]. Oxygen atoms form a slightly distorted square grid, where the bismuth atoms are coordinated above and lower checkered pattern so that each bismuth atom is in vertex of a tetragonal pyramid. $[Bi_2O_2]_n$ plane is divided into strips with the width of four bismuth atoms in the Bi_4BPO_{10} structure (Figs. 5 and 6).

The edge of oxygen "square" in the strip remains incomplete and is compensated by the oxygen atoms of $(PO_4)^{3-}$ anions. Considering the oxygen atoms from anionic groups four types of distorted coordination polyhedrons around Bi can be selected. Bismuth coordination number changes from 5 to 8. Short Bi–O distances are in the range 1.86–2.65 Å (Table 2).

$[BO_3]^{3-}$ anions cross link the parallel strips. The asymmetric coordination of $[BO_3]^{3-}$ anions on top and bottom results in small "bend" of the strips (Figs. 4 and 5). $(PO_4)^{3-}$ anions participate both in strips linking into the stack and in the binding adjacent stacks. These groups are responsible for the shift of adjacent stacks respectively each other.

The reason leading to the fragmentation of infinite plane $[Bi_2O_2]_n$ into the separated strips apparently relates with the chemical composition of the compound. It is well known that highly charged metal ions have no strong polarization feature due to charge compensation mechanism by forming oxygenated cations, e.g., VO_2^+, UO_2^{2+} [31]. The chemical stability of $[Bi_2O_2]_n^{2+}$ plane is supported using similar procedure. In the case of Bi_4BPO_{10} the compensation of bismuth charge is completed by the formation of $[Bi_4O_3]^{6+}$ -charged infinite cationic framework. Apparently $[PO_4]^{3-}$ anion influence on stoichiometry of $[Bi_4O_3]^{6+}$ by attracting oxygens from bismuth oxide. Finally bismuth oxide with a nominal composition of Bi_4O_6 loses 3 oxygen atoms, becoming a cation $[Bi_4O_3]^{6+}$. Lack of oxygen atoms causes the fragmentation of the plane $[Bi_2O_2]_n^{2+}$ into the strips. As a result the structure Bi_4BPO_{10} is constructed from stacks of endless $[Bi_4O_3]$ strips separated by $(BO_3)^{3-}$ and $(PO_4)^{3-}$ anions.

Among the known bismuth borates and phosphates there are no analogues containing layers of $[Bi_2O_2]$. The phase $Bi_4B_2O_9$ is much close in composition to the discussed compound [32]. Borons have similar triangular coordination. However there are no layers of $[Bi_2O_2]$ or fragments thereof in the structure. Layered structures known among dioxo-dibismuth hydroborates $[Bi_2O_2][B_3O_5(OH)]$ and $[Bi_2O_2](BO_2(OH))$ [31].

3.4. Bi_4BPO_{10} electronic band structure modeling

Fig. 7 presents the band electronic structure of Bi_4BPO_{10} obtained by DFT approach. The calculated and experimental absorption spectra are shown in Fig. 8a, b. The obtained forbidden band gap is 3.56 eV. It is rather close to the experimental value of 3.46 eV. The results show that the compound is a direct-gap semiconductor with a band gap minimum in the "gamma" point. Absorption spectrum calculated for different directions of the crystal (Fig. 8) indicates the presence of optical anisotropy, which is the most pronounced along the b axis.

In particular, the difference is in the presence on the calculated spectrum the long-wavelength peak at ~350 nm (3.55 eV) near the absorption edge. This spectral feature can be explained by the orientation of the nonbonding orbitals. An indirect confirmation of their presence in the system is weak dispersion of the top filled band which is absent along other directions. To identify the localization of nonbonding atomic orbitals the state densities were calculated (Fig. 7). The largest contribution to the partial state densities near the Fermi level was made by oxygen and bismuth atoms. The localized $6s^2$ electron pairs and polyhedra type as $EBiO_3$ and $EBiO_4$ (where E – $6s^2$ pair) are often taken into account in

Table 2
The interatomic distances in Bi_4BPO_{10}.

Atom A	Atom B	d(A–B), Å	Atom A	Atom B	d(A–B), Å	Atom A	Atom B	d(A–B), Å
Bi1	O3	2.032(17)	Bi2	O9	2.519(15)	Bi4	O1	2.616(16)
Bi1	O3	2.537(18)	Bi3	O6	2.574(4)	Bi4	O10	2.705(16)
Bi1	O9	2.653(4)	Bi3	O2	2.228(12)	P1	O5	1.52(2)
Bi1	O5	2.617(15)	Bi3	O1	1.858(3)	P1	O7	1.53(4)
Bi1	O1	2.402(17)	Bi3	O4	2.395(16)	P1	O6	1.518(19)
Bi2	O1	2.504(15)	Bi3	O10	2.305(15)	P1	O4	1.51(4)
Bi2	O2	1.897(12)	Bi4	O8	1.859(3)	B1	O8	1.42(2)
Bi2	O7	2.628(15)	Bi4	O3	2.623(4)	B1	O9	1.418(16)
Bi2	O5	2.379(12)	Bi4	O3	2.163(4)	B1	O10	1.42(2)

Table 3
The bond angles in Bi_4BPO_{10}.

Atom A	Atom B	Atom C	Angle (ABC)	Atom A	Atom B	Atom C	Angle (ABC)
Bi1	O3	Bi1	110.09(14)	Bi2	O9	B1	114.3(12)
Bi1	O2	Bi2	115.27(12)	Bi4	O8	B1	110.66(11)
Bi1	O1	Bi2	100.45(10)	Bi3	O10	B1	115.6(12)
Bi1	O3	Bi4	116.28(12)	Bi3	O4	P1	162.23(7)
Bi1	O9	B1	106.72(6)	Bi2	O5	P1	105.0(17)
Bi4	O3	Bi4	106.46(13)	Bi4	O6	P1	121.9(11)
Bi4	O1	Bi3	102.98(12)	Bi2	O7	P1	110.03(6)
Bi4	O2	Bi3	98.8(4)				

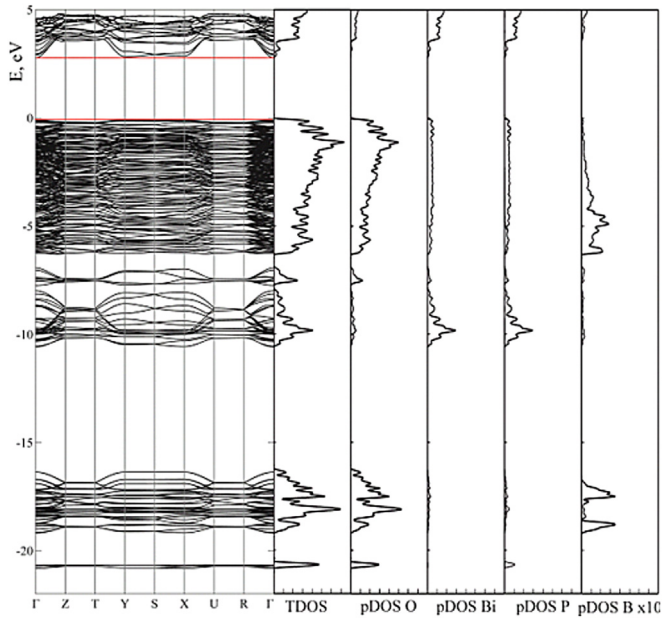

Fig. 7. The electronic band structure, total (TDOS) and partial (pDOS) state density for a single crystal Bi_4BPO_{10}.

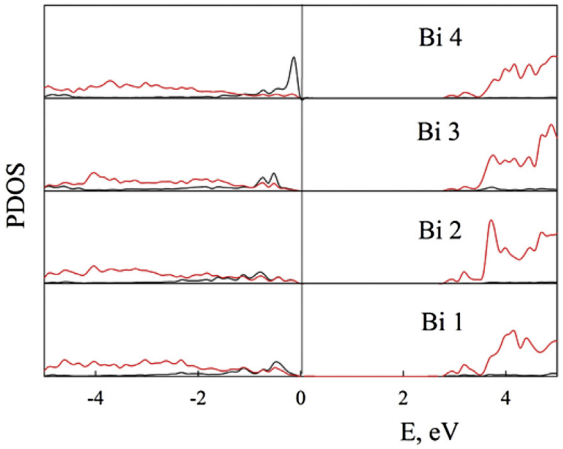

Fig. 9. The partial state densities (pDOS) for s (black lines) and p electrons (red lines) of different bismuth atoms in a single crystal of Bi_4BPO_{10} near the Fermi level. (For interpretation of the references to colour in this figure legend, the reader is referred to the web version of this article.)

describing the bismuth coordination sphere in its oxide phases. Therefore the partial state densities for s- and p-electrons were constructed separately for nonequivalent bismuth atoms (Fig. 9). Analysis of the state densities shows a significant mixing of the contributions from s and p-orbitals of bismuth atoms, indicating their joint hybridization. The exception is the peak of s state for the fourth Bi atom near the Fermi level corresponding to the nonbonding level of $6s^2$ electron pair. In order to clarify the possible orientation of $6s^2$ electron pair the modeling the electron density distribution of the filled band top inside crystal cell of Bi_4BPO_{10} was carried out (Fig. 10). Calculations showed the displacement of the electron density in the localized $6s^2$ pair Bi_4 atom with the formation of polyhedron $EBiO_4$.

4. Conclusion

New bismuth borophosphate Bi_4BPO_{10} was obtained from the stoichiometric melt by spontaneous crystallization approach. At heating the compound is stable up to 812 °C then melts peritectically with decomposition. The crystal structure was determined by

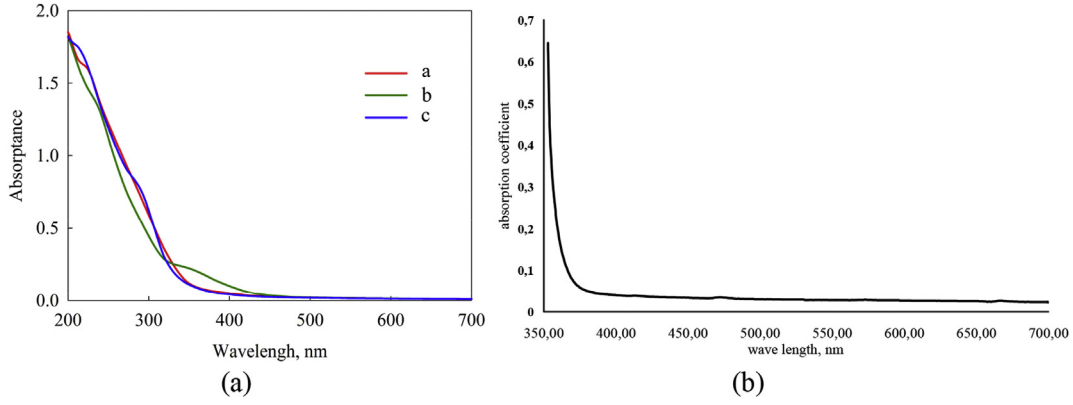

Fig. 8. (a) – Calculated absorption spectra in the directions of the crystallographic axes; (b) – the experimental absorption coefficient of the powder sample for Bi_4BPO_{10}.

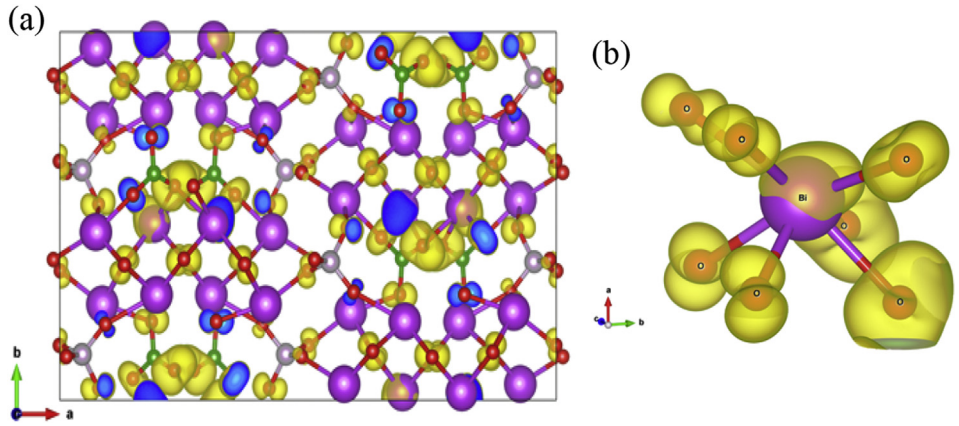

Fig. 10. The electron density distribution for the highest occupied zone in the unit cell (a) and Bi_4 atom in the polyhedron(b).

X-ray powder diffraction technique. The peculiarity of the crystal structure of the compound is in the possibility of separating the anion and cation parts. Bismuth–oxygen cation part with specific composition $[Bi_4O_3]^{6+}$ forms endless strips with 4 bismuth atoms width. The parallel strips are gathered into the stacks and separated in stacks by planar triangular isolated anions $[BO_3]^{3-}$. Tetrahedral anions $[PO_4]^{3-}$ are located between adjacent stacks. The compound is the direct-gap semiconductor. The band gap is defined on the absorption edge in visible spectra equals to 3.46 eV. The band structure modeling by DFT method allowed the calculation of band gap (3.56 eV) rather close to the experimental value. The direction of $6s^2$ electron pair Bi_4 was also calculated.

Acknowledgments

The study was performed with the financial support of the Ministry of Science and Education of the Russian Federation, Projects 3049, 3098, item 1025, “Fund for Assistance to Small Innovative Enterprises in Science and Technology” (Grant program “UMNIK” 2013 II half GU1/2014), ICDD Grant-in-Aid, #93-10.

References

[1] A.V. Egorysheva, V.M. Skorikov, Efficient nonlinear optical material BiB_3O_6 (BIBO), Inorg. Mater. Rus. 45 (2009) 1461–1476.
[2] E.M. Levin, C.L. McDaniel, The system Bi_2O_3–B_2O_3, J. Am. Ceram. Soc. 45 (1962) 355–360.
[3] R. Cong, T. Yang, J. Sun, Y. Wang, J. Lin, Observation of the sixth polymorph of BiB_3O_6: in situ high-pressure Raman spectroscopy and synchrotron X-ray diffraction studies on the β-polymorph, Inorg. Chem. 52 (2013) 7460–7466.
[4] Y.F. Kargin, V.P. Zhereb, A.V. Egorisheva, Phase diagram of the metastable states of the system Bi_2O_3-B_2O_3, J. Inorg. Chem. Rus. 47 (2002) 1357–1359.
[5] V.V. Volkov, L.A. Zhereb, Y.F. Kargin, System $Bi_2O_3 - P_2O_5$, J. Inorg. Chem. Rus. 28 (1983) 1002–1005.
[6] V.P. Zhereb, Y.F. Kargin, L.A. Zhereb, V.A. Mironov, V.M. Skorikov, Stable and metastable equilibrium in the system $Bi_2O_3 - BiPO_4$, Inorg. Mater. Rus. 39 (2003) 1–4.
[7] J.P. Wignacourt, M. Drache, P. Conflant, J.C. Boivin, New phases in Bi_2O_3- $BiPO_4$ system. 1. Description of phase diagram, J. Chim. Phys. 88 (1991) 1933–1938.
[8] V.A. Mironova, Metastable Equilibrium in Systems $Bi_2O_3 - P_2O_5 - E_2O_3$, (E = B, Al, Ga) [PhD Dissertation, Krasnoyarsk], 2000.
[9] L.A. Zhereb, Interactions in the System $Bi_2O_3 - P_2O_5 - E_2O_3$, where E = B, Al, Ga, Fe [PhD Dissertation, Moscow], 1983.
[10] M. Belfaquir, T. Guedira, S. Elyoubi, J. Rehspringer, Synthesis and characterization of some phases of the ternary system Bi_2O_3-P_2O_5-B_2O_3, Ann. de Chimie Sci. des Matériaux 30 (2005) 27–35.
[11] O.A. Gurbanova, E.L. Belokoneva, Comparative crystal-chemical analysis of borosilicates and borophosphates, Crystallogr. Rus. 52 (2007) 651–660.
[12] R. Kniep, H. Engelhardt, C. Hauf, A first approach to borophosphate structural chemistry, Chem. Mater. 10 (1998) 2930–2934.
[13] G. Brower, Inorganic Synthesis Manual, Mir, Moscow, 1985.
[14] J.W. Visser, A fully automatic program for finding the unit cell from powder data, J. Appl. Cryst. 2 (1969) 89–95.
[15] S.D. Kirik, S.V. Borisov, V.E. Fedorov, Program for crystal structure refinement using X-ray powder pattern, Zhurnal Strukt. Khim. Rus. 22 (1981) 131–135.
[16] A. Altomare, R. Caliandro, M. Camalli, C. Cuocci, C. Giacovazzo, A.G.G. Moliterni, R. Rizzi, Automatic structure determination from powder data with *EXPO2004*, J. Appl. Cryst. 37 (2004) 1025–1028.
[17] S.D. Kirik, Refinement of the crystal structures using X-ray the powder pattern profile with rigid structural constraints, Crystallogr. 30 (1985) 185–187.
[18] J. Rodriguez-Carvajal, FullProf Version 4.06, ILL [unpublished].
[19] G. Kresse, J. Hafner, Ab initio molecular dynamics for liquid metals, Phys. Rev. B47 (1993) 558–561.
[20] G. Kresse, J. Hafner, Ab initio molecular-dynamics simulation of the liquid-metal–amorphous-semiconductor transition in germanium, Phys. Rev. B49 (1994) 14251–14269.
[21] G. Kresse, J. Furthmůller, Efficient iterative schemes for ab initio total-energy calculations using a plane-wave basis set, Phys. Rev. B54 (1996) 11169–11186.
[22] P. Hohenberg, W. Kohn, Inhomogeneous electron gas, Phys. Rev. 136 (1964) 864–871.
[23] W. Kohn, L.J. Sham, Self-consistent equations including exchange and correlation effects, Phys. Rev. 140 (1965) 1133–1138.
[24] P.E. Blöchl, Projector augmented-wave method, Phys. Rev. B 50 (1994) 17953–17979.
[25] G. Kresse, J. Joubert, From ultrasoft pseudopotentials to the projector augmented wave method, Phys. Rev. B 59 (1999) 1758–1775.
[26] K. Nakamoto, Infrared and Raman Spectra of Inorganic and Coordination Compounds, New York, 1978.
[27] Infrared Spectra Atlas of Phosphates: Condensed Phosphates, Nauka, Moscow, 1985.
[28] I. Ardelean, S. Cora, R.C. Lucacel, O. Hulpus, EPR and FT-IR spectroscopic studies of B_2O_3–Bi_2O_3–MnO glasses, Solid State Sci. 7 (2005) 1438–1442.
[29] A.V. Egorysheva, V.I. Burkov, Y.F. Kargin, V.G. Plotnichenko, V.V. Koltashev, Vibrational spectra of crystals of bismuth borates, Crystallogr. Rus. 50 (2005) 127–136.
[30] B. Aurivilllius, Mixed bismuth oxides with layer lattices, Arki. Kemi. 54 (1949) 463–527.
[31] S.V. Krivovichev, O. Mentre, O.I. Siidra, M.C. olmont, S.K. Filatov, Anion-centered tetrahedra in inorganic compounds, Chem. Rev. 113 (2013) 6459–6535.
[32] S.K. Filatov, Y.F. Shepelev, Y.V. Aleksandrova, R.S. Bubnova, Structure of bismuth oxoborate $Bi_4B_2O_9$ at 20, 200, and 450 °C, J. Inorg. Chem. Rus. 52 (2007) 21–28.